J|A|C|S COMMUNICATIONS

Published on Web 08/23/2010

Enhanced Electrochemical Lithium Storage by Graphene Nanoribbons

Tarun Bhardwaj,[†] Aleks Antic,[‡] Barbara Pavan,[‡] Veronica Barone,*[,§] and Bradley D. Fahlman*[,†]

Department of Chemistry, Science of Advanced Materials Ph.D. Program, and Department of Physics, Central Michigan University, Mt. Pleasant, Michigan 48859

Received July 19, 2010; E-mail: v.barone@cmich.edu; fahlm1b@cmich.edu

Abstract: Herein, we report the electrochemical Li intake capacity of carbonaceous one-dimensional graphene nanoribbons (GNRs) obtained by unzipping pristine multiwalled carbon nanotubes (MWCNTs). We have found that nanotubes with diameters of ~50 nm present a smaller reversible capacity than conventional mesocarbon microbead (MCMB) powder. Reduced GNRs improve the capacity only marginally over the MCMB reference but present a lower Coulombic efficiency as well as a higher capacity loss per cycle. Oxidized GNRs (ox-GNRs) outperform all of the other materials studied here in terms of energy density. They present a first charge capacity of ~1400 mA h g^{-1} with a low Coulombic efficiency for the first cycle (~53%). The reversible capacity of ox-GNRs is in the range of 800 mA h g^{-1}, with a capacity loss per cycle of ~3% for early cycles and a decreasing loss rate for subsequent cycles.

The development of efficient lithium ion batteries relies on the complex optimization of novel materials for the anode, the cathode, and the electrolyte. The material of choice for the anode in current commercial batteries is graphite, which presents a maximum lithium storage capacity of ~370 mA h g^{-1}. In the pursuit of improvement in this capacity, other carbonaceous materials have been investigated, including carbon nanotubes, graphene oxide sheets, and amorphous carbon.[1−4]

Recently, a single layer of graphite, known as graphene, was synthesized for the first time via mechanical exfoliation of graphite by Novoselov et al.[5] This discovery has ushered in a "graphene frontier", with worldwide interest in exploiting its unique electronic properties for possible applications in energy storage and microelectronics.[6,7] Electrochemical lithium intercalation in graphene nanosheets has been investigated by Yoo et al.[8] and Lian et al.[9] Yoo et al. obtained high reversible capacities that increased to 800 mA h g^{-1} when the graphene layer-to-layer distance was increased by introducing nanotubes and fullerenes between layers.[8] The capacity improvement over graphite discussed above motivates further investigation of other carbon morphologies.

Graphene can also be manipulated to form quasi-one-dimensional strips called graphene nanoribbons (GNRs).[10] The electronic properties of these materials present some similarities to those of single-walled carbon nanotubes (SWCNTs), which have metallic or semiconducting properties that depend on morphology. However, GNRs are further characterized by the presence of edges that govern their electronic behavior through their edge morphology.[11−13]

Although GNRs have received a lot of attention because of their peculiar properties,[12−16] they have never been studied as an electrode material for Li ion batteries. Our recent computational studies predicted that the presence of edges in GNRs would enhance their reactivity toward Li adsorption.[17] Even though experiments are governed by complicated reactions taking place among Li ions, the electrolyte, and the electrode material, it is important to study the effect of edges in the mechanisms of Li intercalation and deintercalation in the carbonaceous electrodes. Herein, we present the first galvanostatic experimental results on electrochemical Li intercalation and deintercalation in GNRs and discuss their reversible and irreversible capacities and cyclability.

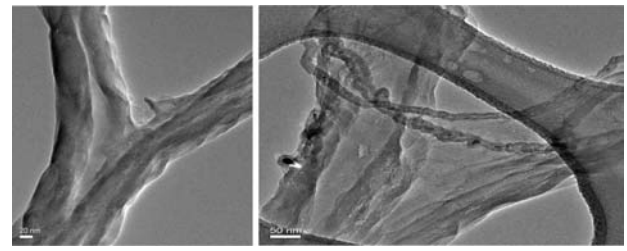

Figure 1. TEM images of partially and fully unzipped MWCNTs.

GNRs were synthesized by unzipping multiwalled carbon nanotubes (MWCNTs) with outer diameters varying from 50 to 80 nm, as reported by Tour and co-workers.[18,19] Figure 1 displays TEM images of unzipped nanoribbons showing that the GNRs retained some curvature due to incomplete unzipping of the MWCNTs. X-ray diffraction data (Figure S1 in the Supporting Information) indicate that this partially unzipped structure is present, on average, in the bulk of the sample. This observation is in line with the local structure revealed by the TEM images and other recent experiments.[20] The present data suggest that GNRs obtained by this method present a nonuniform structure.

The unzipping technique utilizes a solution-based oxidative process to cut the walls of the MWCNTs along their axes. This procedure leaves rows of oxygen-containing groups along the unzipped ribbon edges as well as chemisorbed on the GNR surfaces; the oxidized GNRs will be denoted herein as ox-GNRs. The heavy oxidation in ox-GNRs disrupts the sp^2 hybridization of the carbon lattice, which in turn affects their electronic properties. A simple one-step annealing process was used in order to reduce the ox-GNRs. The as-formed ox-GNRs were placed in a quartz tube and saturated with a 5% H_2/Ar mixture for 15 min. A Thermolyne 79300 tube furnace was used to heat the GNRs to 900 °C in the same 1:1 mixture of argon and hydrogen used in the pregassing step, after which the furnace was shut off and the GNRs were allowed to cool to room temperature under the gas mixture to prevent reoxidation. It should be noted that we did not observe any morphological differences between oxidized and reduced GNRs, analogous to other reports.[18,19]

MWCNTs were evaluated by elemental analysis as-received from the vendor as well as after unzipping both before and after the reduction process in order to determine hydrogen, carbon, and

[†] Department of Chemistry.
[‡] Science of Advanced Materials Ph.D. Program.
[§] Department of Physics.

 10.1021/ja106162f

Scheme 1. Illustration of the Surface Composition of GNRs before and after Reduction (Passivating H Atoms Have Been Omitted for Clarity)

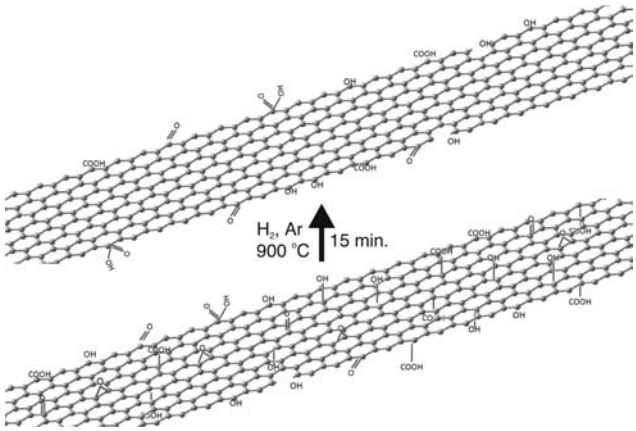

oxygen atomic percentages. Prior to treatment, MWCNTs consisted of 97% carbon. After the MWCNTs were unzipped, the resulting ox-GNRs consisted of 46% carbon, 25% hydrogen, and 25% oxygen. After reduction, the reduced GNRs consisted of 97% carbon, with the amounts of H and O below the detection limits of the elemental analyzer. This may be compared to the work of Kosynkin et al.,[18] who reported the use of a more complicated solution-based hydrazine reduction procedure to yield oxygen atomic concentrations of 41.8 and 16.1% for oxidized and reduced GNRs, respectively.

The Raman spectra of the nanoribbons (reduced and oxidized) are mostly characterized by the relative increase of the D band over the G band and the disappearance of the peak at ~2600 cm^{-1} (Figure S2, in the Supporting Information), in agreement with previous results. In accord with other reports for graphite oxide,[21] the IR spectrum of ox-GNRs shows peaks at 3359 cm^{-1} (−OH), 1714 cm^{-1} (−C═O), 1392 cm^{-1} (C−O, carboxy), 1219 cm^{-1} (C−O, epoxy), and 1030 cm^{-1} (C−O, alkoxy), whereas the spectrum for reduced GNRs is featureless (Figure S3, in the Supporting Information). After reduction, the only −H/−O moieties present should be bound to the edge sites (Scheme 1).[22] Since our nanoribbons were relatively wide (200−400 nm), the edge-C/surface-C ratio was extremely small, resulting in a proportion of −H groups that was undetectable by IR spectroscopy and below the detection limits for elemental analysis.

A slurry was prepared by mixing 85% active electrode material, 10% poly(vinylidine difluoride) (PVDF) binder (Sigma-Aldrich), and 5% carbon black in 1-methyl-2-pyrrolidinone (NMP) solvent supplied by Sigma-Aldrich. Electrodes were fabricated by coating a slurry of carbon materials on Cu foil; typically, 1−3 mg of slurry was coated on Cu foil (1 cm^2 × 0.001 in. thickness) and dried overnight at 110 °C under an Ar atmosphere.

All of the electrochemical experiments were performed inside an Ar atmosphere MBRAUN Labstar glovebox with moisture and oxygen levels below 0.1 ppm. A VersaStat3 potentiostat/galvanostat (Princeton Applied Research) was used to perform all of the experiments, which were controlled by VersaStudio software. A STC 20-split flat cell (MTI Corp., Richmond, CA) was used for the present studies. Lithium foil with a thickness of 0.05 mm (GoodFellow Corp.) was used for the counter and reference electrodes. A 25 μm polyethylene separator (MTI Corp.) was used between the two electrodes. The electrolyte used in the experiments was 1 M $LiPF_6$ in 1:1:1 EC/DMC/DEC supplied by MTI Corp.

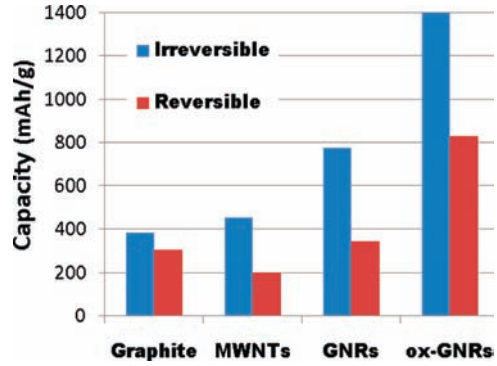

Figure 2. First cycle reversible and irreversible capacities of MCMB graphite, multiwalled carbon nanotubes, reduced GNRs, and oxidized GNRs.

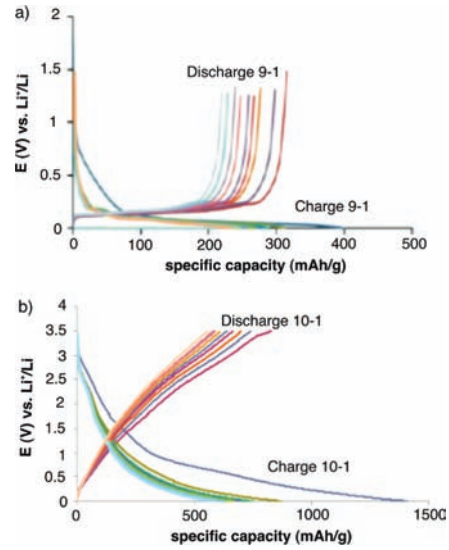

Figure 3. Charge/discharge profiles for (a) MCMB graphite and (b) ox-GNRs.

For benchmark experiments, graphite in the form of mesocarbon microbead (MCMB) grade (Pred Materials, New York, NY) was used.

Galvanostatic charge and discharge experiments were conducted at a C/10 rate (i.e., 10 h for a half-cycle charge/discharge) over the potential range 0.0−3.5 V versus Li^+/Li. The current density was set at 0.1 mA/cm^2. In Figure 2, we present the first charge and discharge specific capacities for the different materials studied here. MWCNTs present a higher first charge capacity than MCMB graphite. However, this capacity is mostly irreversible, and its reversible capacity, which is of interest for battery applications, is only ~200 mA h g^{-1}, in agreement with previous experiments.[23,24] Reduced GNRs improve both the first charge and discharge capacities with respect to MWNTs, but their reversible capacity is just slightly higher than in the conventional graphite electrode. Notably, ox-GNRs present much higher specific capacities. The first charge capacity is 1400 mA h g^{-1}, although at discharge only 820 mA h g^{-1} is recovered (Figure 3). The increase in both reversible and irreversible capacities in ox-GNRs suggests that the presence of oxygen in GNRs induces the formation of a much more stable, chemically bonded solid electrolyte interface (SEI).[25−27] This Li-rich robust SEI likely prevents electrode degradation and enhances the Li exchange and storage capacity of the electrode.

While the Coulombic efficiency (CE) of MCMB graphite is ~75% in the first cycle and ~90% in the following cycles, the

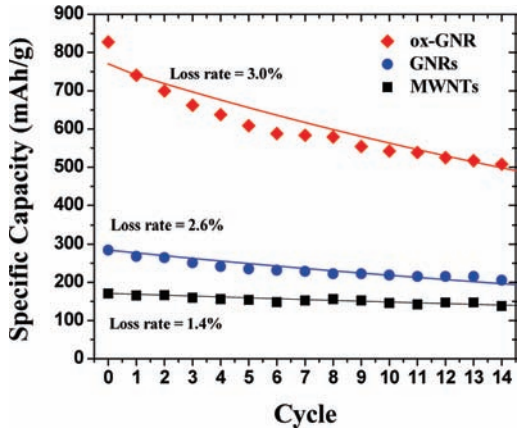

Figure 4. Cyclability of three different carbonaceous electrode materials. Symbols represent experimental measurements, while bold lines represent values extrapolated at the indicated loss rates.

CEs of the studied nanomaterials are as follows: MWCNTs present a CE of 44% for the first cycle and ~85% for the remaining cycles; GNRs exhibit a CE that is very similar to MWNTs (45% in the first cycle and ~88% in the remaining cycles). In contrast, ox-GNRs perform better in terms of CE, presenting a 53% efficiency during the first cycle and ~95% for subsequent cycles.

Another useful parameter for battery cyclability is the capacity loss per cycle, which relates the reversible capacity of a given cycle with the reversible capacity in the immediate previous cycle. The average capacity loss is ~1.4% for MWNTs, 2.6% for GNRs, and 3.0% for ox-GNRs. Therefore, MWNTs perform better than GNRs and ox-GNRs in terms of cyclability. If we assume a constant capacity loss for each material, it is possible to extrapolate the capacity as a function of cycle number using the following relation:

$$C_n = C_0(1 - x)^n \qquad (1)$$

where C_0 and C_n are the capacities in the first and n^{th} cycles, respectively, and x is the capacity loss of the specific material. In Figure 4, we present the cycling results for MWCNTs, GNRs, and ox-GNRs. Symbols represent the experimental data, while bold lines represent the extrapolated results obtained using eq 1. With this extrapolation, it is expected that under the same ambient conditions, the capacity of MWNTs after 50 cycles should be ~45% of that of first cycle, while for the ox-GNRs, the capacity after 50 cycles should be just 19% of the first-cycle capacity. However, from the curves in Figure 4, it seems that ox-GNRs stabilize their capacity loss rate more slowly than MWNTs, so the 3.0% loss rate is reduced in subsequent cycles. For instance, if one considers the specific capacities over cycles 3−14 (after the initial SEI-induced drop), the average loss rate is only 2.3%.

In summary, we have studied the electrochemical Li intake capacity of carbonaceous one-dimensional materials including multiwalled carbon nanotubes and GNRs obtained by unzipping the MWCNTs. We have found that nanotubes with diameters of ~50 nm present a smaller reversible capacity than conventional MCMB graphite. Reduced GNRs improve the capacity only marginally over MCMB graphite but present a lower Coulombic efficiency as well as a higher capacity loss per cycle. Oxidized GNRs outperform all of the other materials studied here in terms of energy density. They present a first charge capacity of ~1400 mA h g^{-1} with a low Coulombic efficiency for the first cycle (~53%). The reversible capacity of ox-GNRs is in the range of 800 mA h g^{-1}, with a capacity loss per cycle of ~3% for early cycles and a decreasing loss rate for subsequent cycles.

Acknowledgment. This work was funded by TARDEC/ARO under Subcontract Agreement TCN09227. We acknowledge Professor Valeri Petkov in the Department of Physics at Central Michigan University (CMU) for providing XRD data. We also thank Dr. Xudong Fan at the Center for Advanced Microscopy at Michigan State University and Phil Oshel in the Biology Department at CMU for their assistance with EM characterization of our nanoribbons.

Supporting Information Available: Raman and IR spectra and XRD data. This material is available free of charge via the Internet at http://pubs.acs.org.

References

(1) Gao, B.; Kleinhammes, A.; Tang, X. P.; Bower, C.; Fleming, L.; Wu, Y.; Zhou, O. *Chem. Phys. Lett.* **1999**, *307*, 153–157.
(2) Li, H.; Wang, Z. X.; Chen, L. Q.; Huang, X. J. *Adv. Mater.* **2009**, *21*, 4593–4607.
(3) Liang, M. H.; Zhi, L. J. *J. Mater. Chem.* **2009**, *19*, 5871–5878.
(4) Pan, D. Y.; Wang, S.; Zhao, B.; Wu, M. H.; Zhang, H. J.; Wang, Y.; Jiao, Z. *Chem. Mater.* **2009**, *21*, 3136–3142.
(5) Novoselov, K. S.; Geim, A. K.; Morozov, S. V.; Jiang, D.; Zhang, Y.; Dubonos, S. V.; Grigorieva, I. V.; Firsov, A. A. *Science* **2004**, *306*, 666–669.
(6) Neto, A. H. C.; Guinea, F.; Peres, N. M. R.; Novoselov, K. S.; Geim, A. K. *Rev. Mod. Phys.* **2009**, *81*, 109.
(7) Rao, C. N. R.; Sood, A. K.; Subrahmanyam, K. S.; Govindaraj, A. *Angew. Chem., Int. Ed.* **2009**, *48*, 7752.
(8) Yoo, E.; Kim, J.; Hosono, E.; Zhou, H.; Kudo, T.; Honma, I. *Nano Lett.* **2008**, *8*, 2277–2282.
(9) Lian, P. C.; Zhu, X. F.; Liang, S. Z.; Li, Z.; Yang, W. S.; Wang, H. H. *Electrochim. Acta* **2010**, *55*, 3909–3914.
(10) Berger, C.; Song, Z. M.; Li, X. B.; Wu, X. S.; Brown, N.; Naud, C.; Mayou, D.; Li, T. B.; Hass, J.; Marchenkov, A. N.; Conrad, E. H.; First, P. N.; de Heer, W. A. *Science* **2006**, *312*, 1191–1196.
(11) Fujita, M.; Wakabayashi, K.; Nakada, K.; Kusakabe, K. *J. Phys. Soc. Jpn.* **1996**, *65*, 1920–1923.
(12) Hod, O.; Barone, V.; Peralta, J. E.; Scuseria, G. E. *Nano Lett.* **2007**, *7*, 2295–2299.
(13) Barone, V.; Hod, O.; Scuseria, G. E. *Nano Lett.* **2006**, *6*, 2748–2754.
(14) Son, Y. W.; Cohen, M. L.; Louie, S. G. *Phys. Rev. Lett.* **2006**, *97*, 216803.
(15) Han, M. Y.; Özyilmaz, B.; Zhang, Y. B.; Kim, P. *Phys. Rev. Lett.* **2007**, *98*, 206805.
(16) Wang, X. R.; Ouyang, Y. J.; Li, X. L.; Wang, H. L.; Guo, J.; Dai, H. J. *Phys. Rev. Lett.* **2008**, *100*, 206803.
(17) Uthaisar, C.; Barone, V.; Peralta, J. E. *J. Appl. Phys.* **2009**, *106*, 113715.
(18) Kosynkin, D. V.; Higginbotham, A. L.; Sinitskii, A.; Lomeda, J. R.; Dimiev, A.; Price, B. K.; Tour, J. M. *Nature* **2009**, *458*, 872–876.
(19) Higginbotham, A. L.; Kosynkin, D. V.; Sinitskii, A.; Sun, Z.; Tour, J. M. *ACS Nano* **2010**, *4*, 2059–2069.
(20) Sinitskii, A.; Fursina, A. A.; Kosynkin, D. V.; Higginbotham, A. L.; Natelson, D.; Tour, J. M. *Appl. Phys. Lett.* **2009**, *95*, 253108.
(21) Park, S.; Dikin, D. A.; Nguyen, S. T.; Ruoff, R. S. *J. Phys. Chem. C* **2009**, *113*, 15801–15804.
(22) Xiang, H.; Kan, E.; Wei, S.-H.; Whangbo, M.-H.; Yang, J. *Nano Lett.* **2009**, *9*, 4025–4030.
(23) Yang, S. B.; Huo, J. P.; Song, H. H.; Chen, X. H. *Electrochim. Acta* **2008**, *53*, 2238–2244.
(24) Landi, B. J.; Dileo, R. A.; Schauerman, C. M.; Cress, C. D.; Ganter, M. J.; Raffaelle, R. P. *J. Nanosci. Nanotechnol.* **2009**, *9*, 3406–3410.
(25) Chusid, O.; Ely, Y. E.; Aurbach, D.; Babai, M.; Carmeli, Y. *J. Power Sources* **1993**, *43*, 47–64.
(26) Peled, E.; Menachem, C.; BarTow, D.; Melman, A. *J. Electrochem. Soc.* **1996**, *143*, L4–L7.
(27) Menachem, C.; Peled, E.; Burstein, L.; Rosenberg, Y. *J. Power Sources* **1997**, *68*, 277–282.

JA106162F